Morphological effects of nanosecond- and femtosecond-pulsed laser ablation on human middle ear ossicles

Justus Ilgner
RWTH Aachen University Hospital
Department of Otorhinolaryngology
Plastic Head and Neck Surgery
Pauwelsstrasse 30
52057 Aachen, Germany
E-mail: jilgner@ukaachen.de

Martin Wehner
Fraunhofer Institute for Lasertechnology (ILT)
Steinbachstrasse 15
52074 Aachen, Germany

Johann Lorenzen
Manfred Bovi
RWTH Aachen University Hospital
Institute of Pathology Pauwelsstrasse 30
52057 Aachen, Germany

Martin Westhofen
RWTH Aachen University Hospital
Department of Otorhinolaryngology
Plastic Head and Neck Surgery
Pauwelsstrasse 30
52057 Aachen, Germany

Abstract. We evaluate the feasibility of nanosecond-pulsed and femtosecond-pulsed lasers for otologic surgery. The outcome parameters are cutting precision (in micrometers), ablation rate (in micrometers per second), scanning speed (in millimeters per second), and morphological effects on human middle ear ossicles. We examine single-spot ablations by a nanosecond-pulsed, frequency-tripled Nd:YAG laser (355 nm, beam diameter 10μm, pulse rate 2 kHz, power 250 mW) on isolated human mallei. A similar system (355 nm, beam diameter 20μm, pulse rate 10 kHz, power 160–1500 mW) and a femtosecond-pulsed CrLi:SAF-Laser (850 nm, pulse duration 100 fs, pulse energy 40 μJ, beam diameter 36 μm, pulse rate 1 kHz) are coupled to a scanner to perform bone surface ablation over a defined area. In our setups 1 and 2, marginal carbonization is visible in all single-spot ablations of 1-s exposures and longer: With an exposure time of 0.5 s, precise cutting margins without carbonization are observed. Cooling with saline solution result is in no carbonization at 1500 mW and a scan speed of 500 mm/s. Our third setup shows no carbonization but greater cutting precision, although the ablation volume is lower. Nanosecond- and femtosecond-pulsed laser systems bear the potential to increase cutting precision in otologic surgery. [DOI: 10.1117/1.2166432]

Keywords: otologic surgical procedures; otolaryngology; otosclerosis; stapes surgery; neodymium; laser surgery.

Paper 05175R received Jul. 2, 2005; revised manuscript received Sep. 25, 2005; accepted for publication Sep. 26, 2005; published online Jan. 24, 2006. This paper is a revision of a paper presented at the SPIE conference on Advances in Otorhinolaryngology: Lasers, Radiofrequency, and Related Technology, January 2004, San Jose, California. The paper presented there appears (unrefereed) in SPIE Proceedings, Vol. 5312.

1 Introduction

Microscopic surgery of middle ear structures requires minimal trauma to the tissue involved to preserve hearing and to avoid damage to the vestibular organ and the facial nerve. In otosclerosis, a condition in which the annular ligament suspending the stapes footplate in the oval niche is fixed, stapedotomy is performed to replace the stapes with a prosthesis joined to the incus, while the distal end is coupled to the inner ear by fenestrating the stapes footplate. This requires precise perforation of the stapes footplate, which is best accomplished by a no-touch technique. Thus, lasers have been introduced to stapes surgery at an early stage. First experimental results with an Nd:YAG laser were published in 1967 by Sataloff.[1] The first clinical use of an Argon laser for stapedotomy was published by Palva[2] and by Perkins.[3] Since then, various lasers, such as the Argon,[4–7] the CO_2 (Refs. 7–12), the KTP (Refs. 7 and 13–18), and the Erbium:YAG (Refs. 19 and 23) have been used in *in vitro* and *in vivo* settings, while the Er:YSGG (Refs. 24 and 25), Holmium:YAG (Refs. 24 and 26), the Xe:Cl (excimer) (Ref. 24), and the diode laser[27] have been evaluated *in vitro* only. The variety of laser systems in use reflects the fact that many of the present systems are suitable but none possesses ideal properties for middle ear applications. In particular, the fact that laser energy in the visible light range, as emitted by the Argon (518 nm) and KTP (532 nm), is absorbed only very little by clear fluid has raised concerns on heating of inner ear structures, such as the perilymph,[12,18,28] the facial nerve, or unwanted irradiation of the saccular macula, a part of the vestibular organ that is situated in direct line about 1.7 to 2.1 mm behind the stapes footplate.[29] On the other hand, as CO_2 laser energy is readily absorbed by fluids, the amount of temperature rise of the perilymph itself and its impact on inner ear function has been subject to further investigations.[16,28,30] While CO_2 lasers operated in cw mode were shown to perform stapedotomy procedures safely, there has been an issue with CO_2 lasers operating in the so-called superpulse mode, as this entails pressure transients that are potentially harmful to the sensory compound action potential of the outer and inner hair cells.[30–32]

Address all correspondence to Justus Ilgner, RWTH Aachen University Hospital, Department of Otorhinolaryngology, Plastic Head and Neck Surgery, Pauwelsstrasse 30, 52057 Aachen, Germany. Tel.: ++49–241–80–88946; Fax: ++49–241–80–82523; E-mail: jilgner@ukaachen.de

1083-3668/2006/11(1)/014004/7/$22.00 © 2006 SPIE

Photoablative systems such as the Er:YAG laser cause little thermal effects and are able to ablate bone in a precise and bloodless manner, but create pressure transients which could result in acoustic trauma.[19,20,31] However, even with a great number of pitfalls, laser surgery of the stapes footplate has been proven to be beneficial in terms of hearing outcome compared to mechanical drilling[11,32] in primary surgery and even more in revision surgery, as the diseased ear is even more vulnerable to mechanical stress induced by conventional surgery.[17,33] In some cases, revision surgery has been made possible only with a laser that otherwise would have been contraindicated.[17] As the dilemma between thermal load and mechanical stress remains unsolved, the safety of laser surgery for the middle ear has been accomplished by (1) meticulous choice of laser parameters,[32,34] (2) surgical techniques which aim to spare structures at risk (e.g., avoiding irradiation of the open vestibule,[18,34] and (3) development of purpose-built instruments that help surgeons to handle the laser beam more precisely[5,32,35,36] (Endo-Otoprobe™, scanning devices, etc.).

Thus, the quality of laser surgery in terms of precision and limitation of possible side effects is largely dependent on the surgeon's skills, as the dilemma between unwanted thermal effects and pressure transients in laser surgery for the ear remains unsolved. Pulsed laser systems working within the nanosecond to femtosecond range seem to show a way out of this dilemma, as they provide pulses that do not induce high-pressure transients in the perilymphatic fluid and that cause little thermal effects.[37–39] This is a major advantage over earlier, e.g., CO_2 pulsed laser systems, whose so-called "ultrapulse" mode (Refs. 30–32) is entirely different from the ultrashort pulsed systems that are now available. Since the required energy for ablation or photodisruption decreases with pulse length,[40,41] side effects such as excess heating of surrounding tissue and disruption by pressure waves can be reduced markedly. The ultrashort pulses emitted by femtosecond lasers result in multiphoton absorption, which creates a plasma field around the target site whose free electrons absorb most of the laser energy. As linear energy absorption by the target tissue itself plays only a minor role, the ablation process depends only weakly on tissue characteristics. Earlier studies performed by Neev et al. on human nail tissue[37] demonstrated a better cutting precision of a Ti:sapphire system compared to Er:YAG, Ho:YSGG, and Xe:CL (excimer) lasers, though ablation rates were inferior. Armstrong et al.[38] were the first to use a Ti:sapphire system for ablation of ossicular tissue in human cadaveric bone and obtained an ablation rate of 1.26 μm/pulse at a repetition rate of 10 Hz. Schwab et al.[39] reported an ablation rate of their Ti:sapphire laser system in relation to varying pulse energy values with a minimal ablation of 20 nm at 22 μJ. Increased precision is beneficial in stapes surgery, as an exact fit of the prosthesis to the perforation helps to avoid leakage of perilymph from the inner ear. Furthermore, with precise bone ablation it is possible to create microstructures in the ossicular chain, which can accommodate bioactive nanolayers, e.g., for the modulation of cell growth around the prosthesis.

We examined the feasibility of a frequency-tripled Nd:YAG laser system at 355 nm working with nanosecond pulses and compared it to an equally experimental setup of a CrLiSAF laser emitting femtosecond pulses at 850 nm. As a reference, a conventional microscope-coupled single-pulsed Er:YAG laser emitting at 2940 nm was used.

The first hypothesis for our considerations is that the optical complexity—and therefore the manufacturing effort—of frequency-tripled Nd:YAG lasers is low compared to ultrafast or femtosecond lasers and a 20-μm resolution can be achieved with relatively simple transmissive optical elements, which, if compared to more complex femtosecond setups, makes such systems attractive for cost-effective microscope-laser units in middle ear microsurgery. The second hypothesis is that both the nanosecond-pulsed, frequency-tripled Nd:YAG laser, and the femtosecond-pulsed CrLiSAF laser, both in conjunction with a scanning system, provide a better ablative precision at little thermal stress and a lower risk of acoustic trauma compared to a manually steered Er:YAG laser system.

2 Material and Methods

We harvested two human mallei, three inci, and one stapes from two postmortem individuals via an intraauricular approach, exposing the middle ear ossicles while leaving the tympanic membrane intact. In both cases, no sign of chronic inflammation or malformation was found. These ossicles were immersed in 3.5% formaldehyde solution for storage.

Principal outcome parameters for each experiment were cutting precision (in micrometers), ablation rate (in micrometers per second), scanning speed (in millimeters per second), and morphological effects on the human ossicular chain. For qualitative evaluation concerning carbonization and denaturation of adjacent bone, light microscopic photographs were taken. The light microscopic focus was used to measure ablation depth in the scanning experiments with an error of ± 2 μm, while the focusing error was approximately ± 5 μm. In addition, quantitative assessment of carbonization margins in a series of singular pulses as well as in all scanning experiments was performed via environmental scanning electron microscopy (ESEM) in gaseous secondary electron emission (GSE) mode (model XL 30 ESEM FEG, FEI/Philips, Eindhoven, Netherlands).

The first laser system consisted of a nanosecond-pulsed, frequency-tripled Nd:YAG laser operating at a 355-nm wavelength (Lambda Physik "Starline," Göttingen, Germany), with a pulse duration of 10 ns full width half maximum (FWHM), a pulse repetition rate of 2 kHz, and pulse energy of 0.125 mJ, resulting in an output power of 250 mW. The beam was focused by a fixed beam-steering system and a microscope objective to a spot of approximately 10 μm diameter. Hence the peak fluence in the center of the spot approached 320 J/cm^2. An x-y translation stage was used to move the mallei into an appropriate position. In a first experiment, ablation characteristics of the bony malleus surface in single spots were examined. In the following, this setup is referred to as "THG-1."

In the second experiment, a frequency-tripled Nd:YAG laser with slightly longer pulse duration of 40 ns FWHM was used (model 210S-355-5000, ILX Lightwave, Bozeman, Montana, USA) and the laser was coupled to a scanner, irradiating four malleus areas of 1×1 mm^2 in meandering courses with a repetition rate of 10 kHz (Fig. 1). Each site

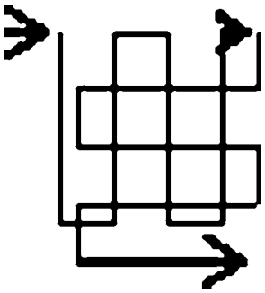

Fig. 1 Scanning course as performed in experiments THG-2, fs 2, and fs 4.

was treated by 28 subsequent courses covering the whole area. The beam diameter in each case was 20 μm. This setup will be referred to as THG-2. The parameters for the different scans are listed in Table 1.

Both lasers emit in transverse electromagnetic mode (TEM_{00})($M^2 < 1.2$) with Gaussian intensity distribution and, for convenience, the peak fluence in the center of the spot is taken as a characteristic.

For the third experiment, we chose human inci whose structure is comparable to those of the mallei used in experiment THG-1 and THG-2. In this case, a femtosecond-pulsed laser system, consisting of a CrLiSAF oscillator and a Colquerite amplifier, emitting at $\lambda = 850$ nm with a bandwidth of 26 nm FWHM was used. The laser spot was focused to a beam diameter of 36 μm. Pulse duration was 100 fs at a repetition rate of 1 kHz and pulse energy of 40 μJ. In that case, the femtosecond-pulsed laser was coupled into a microscope equipped with a motorized stage, which was programmed to irradiate the bony incus surface along the same course as in THG-2 (Fig. 1). The inci were referred to as "fs 2" and "fs 4." Both were exposed to scanning courses with a beam velocity of 2 mm/s in parallel tracks with a mean distance of 10 μm for a 0.4- $\times$ 0.4-mm^2 surface, which resulted in an ablation depth of approximately 40 μm and a scanning time of 40 s/course. The first incus, referred to as fs 2 was exposed to one and three courses respectively, while 10 courses were applied to the incus labeled fs 4.

As a reference, a human stapes was exposed to single pulses of a conventional Er:YAG laser, which was coupled to an operating microscope (Zeiss Opmi ORL E, Zeiss Company, Oberkochen, Germany). The Er:YAG laser operates at a wavelength of $\lambda = 2940$ nm with a beam diameter of 380 μm at a fixed microscope focus of 300 mm, while the pulse duration varies between 50 and 500 μs, depending on the pulse energy. Exposures were performed as follows: 1 pulse at 10 mJ, 1 pulse at 25 mJ, and a series of 49 singular pulses of 15 mJ each with a total energy of 735 mJ to obtain a perforation of 400 μm in diameter, which would be required to insert the stapes prosthesis.

Table 1 Laser parameters for the scanning series performed with setup THG 2.

Scan No.	Power (W)	Pulse Energy (mJ)	Fluence (J/cm^2)	Velocity (mm/s)	Scan Time (s)
1	0,8	0,08	51	200	20
2	0,16	0,016	10.2	200	20
3	1,5	0,15	95,4	500	8
4	1,5	0,15	95,4	500	8

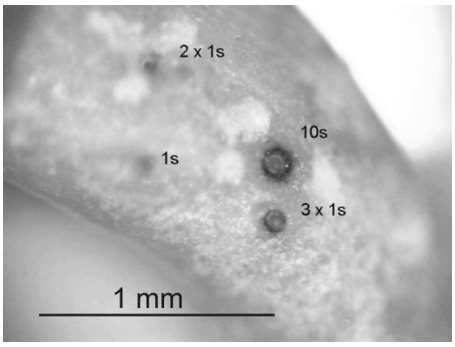

Fig. 2 Single spots with irradiation times of 1 s, 2 $\times$ 1 s, 3 $\times$ 1 s, and 10 s. (Setup THG-1).

3 Results

First, setup and parameter settings THG-1 were used to study the effect of single-spot irradiation when various exposure times were applied to the long malleus process (Fig. 2). With a constant beam diameter of 10 μm, we could observe zones of carbonization, whose width increased with the total exposure time. As there was no coolant applied during these experiments, the findings suggest that excessive heating results in thermal damage, depending on the total energy applied. Prolonging exposure time from 1 to 10 s, the overall crater diameter increased from about 30 to 60 μm, which is considerably wider than the original beam diameter of 10 μm. The carbonization margin increased from less than 10 μm width in the 1-s exposure to about 30 μm in the 10-s exposure. In the 10-s exposure, the full thickness of the malleus process (900 μm) was penetrated. When an exposure time of 0.5 s was chosen (Fig. 3), the ablation diameter was reduced to

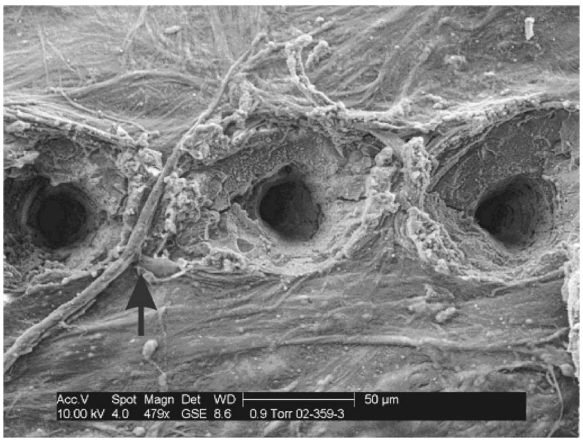

Fig. 3 Single-spot series with exposure times of 0.5 s each. Besides a zone of approx. 10 μm width, suggesting debris, tissue structures appear unchanged (arrow). (Setup THG-1).

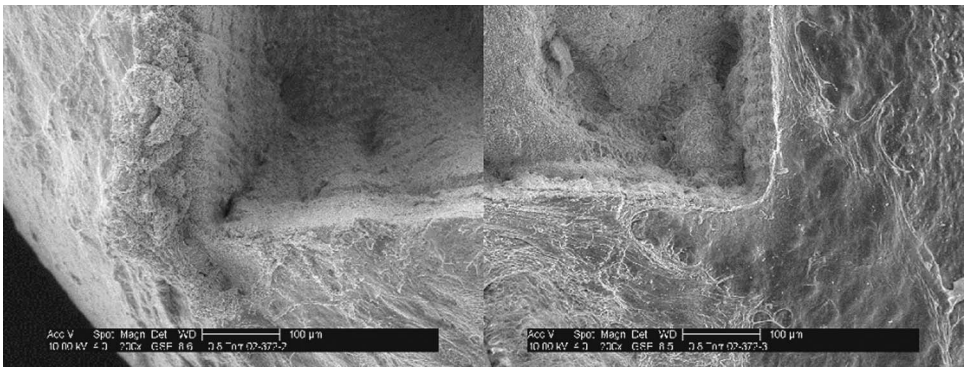

Fig. 4 Scanning series, scan no. 1 (left) and no. 2 (right). From scan no. 1 a zone of denaturated fibrous tissue with a maximum width of 100 μm was observed. Scan No. 2 did not produce any discernible debris. (Setup THG-2).

20 μm with a superficial conical crater of 80 μm diameter. With these parameters, a margin of superficial debris with a width of 10 μm or less was observed. Between adjoining ablation margins, fibrous structures on the surface appeared morphologically intact.

Larger areas of approximately 1-$\times$1-mm^2 size were treated by performing scanning experiments according to setup THG-2. Here, we could observe a debris zone of less than 100 μm width (Fig. 4) adjacent to the ablation crater. Otherwise, scanning electron microscopy revealed no sign of further protein or bone denaturation beyond the debris margin. The crater margins showed a consistent width over all ablated tissue layers. Furthermore, there was mild carbonization at the bottom of the ablated region. Another scan, which was performed at 20% of the power and energy rating of the first, showed no carbonization or collagen denaturation on the bony surface at all, while ablation margins were equally sharp-edged. However, ablation depth was limited while the crater bottom was irregularly shaped. No cooling was used in both experiments.

In contrast, scanning experiment no. 4 was performed under superficial application of 0.9% saline solution (Fig. 5). A drop of saline solution had been applied to the bone and after diffuse moistening of the surface the scanning started. Although power rating was twice as high as in scan no. 1, there was no sign of thermal damage, only a 50-μm margin of fibrous tissue layer detached form the malleus process. The ablation depth extended to 900 μm, which eventually resulted in a full thickness cut through the malleus process. The cutting margin revealed intact Haversian canals with no further signs of bone damage.

With the femtosecond-pulsed CrLiSAF Laser scans, a singular scan with an ablation depth of 40 μm (Fig. 6, right) did not produce any visible debris. In contrast to the low-powered scan no. 2 performed with the frequency-tripled Nd:YAG laser, the base of the ablated area showed a more regular shape. This was also the case with three consecutive scans (Fig. 6, left), while the ablation margins showed some conical shape. However, next to the margins there was a debris zone with a maximum width of 80 μm. In the series of 10 consecutive scans performed with fs-4 (Fig. 7), this debris also had a maximum width of 80 μm, suggesting that it consists of layers of loose material following photoablation rather than a coagulation zone which would be expected to have an increasing width with longer exposure. Cooling was not performed during any of the femtosecond scans.

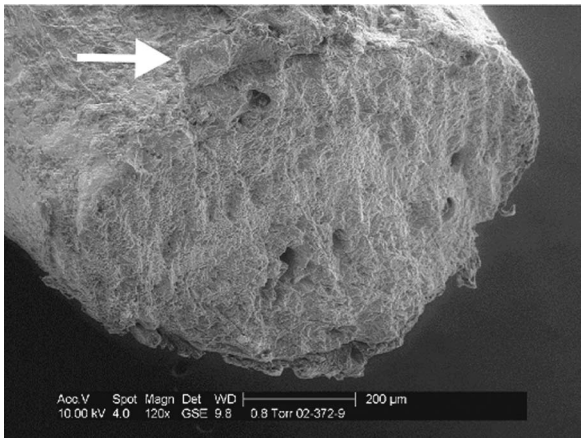

Fig. 5 Through-cut after damping (scanning series no. 4). Lateral aspect of the cutting surface. Detached layer of fibrous tissue (arrow). (Setup THG-2).

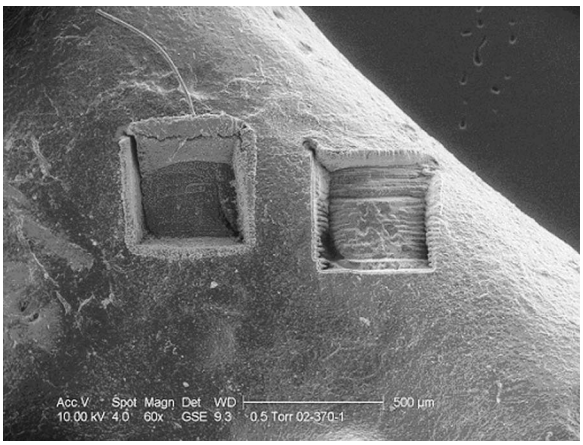

Fig. 6 Areas of 400$\times$400 μm scanned with the femtosecond-pulsed CrLiSAF laser (fs-2). Three consecutive scan courses resulted in an ablation depth of 110 μm (left), while one course created a shallow excavation of 40 μm depth (right).

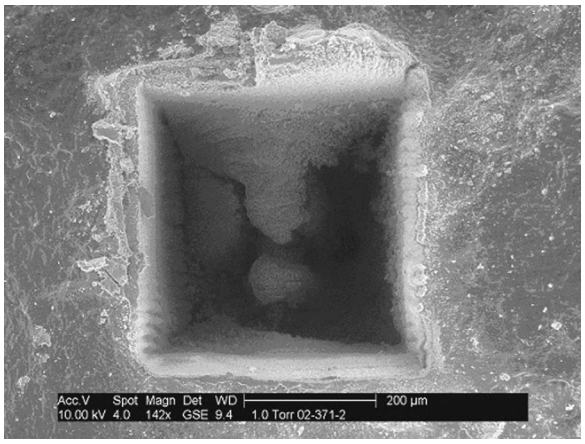

Fig. 7 Same setup as in Fig. 6; 10 courses resulting in an ablation depth of approx. 300 to 360 μm (fs-4).

As expected with the oligothermic ablation properties of the Er:YAG laser, ESEM revealed no visible coagulation in the reference experiment concerning the stapes footplate, while a coagulation zone of very few micrometers cannot be avoided even under optimum ablation conditions. However, given the relatively large beam diameter of 350 μm, ablation took place in shallow excavations of bony material, as seen with the singular pulses of 10 and 25 mJ (Fig. 8). Although saline solution was applied to the stapes footplate at the beginning of the perforation in ablation no. 3, the ablation margins were considerably larger than the actual perforation, which is partially due to the manual steering by means of the micromanipulator, but is also due to a dehydration of the tissue during the laser ablation process, which in turn resulted in a reduced ablation efficiency.

4 Discussion

Regarding the morphological findings in these series, it must be taken into account that all ossicles were immersed in 3.5% formaldehyde solution, which results in some alteration in the fibrous tissue layers. As the material had to be stored before setting up the laser experiments, preference was given to fixed material rather than native ossicles. The data suggest that nanosecond-pulsed tissue ablation at a wavelength of 355 nm does result in mild molecular interaction in terms of protein denaturation or photocoagulation. However, this effect is strongly dependent on the exposure time and relatively minor compared to ablation depth in a single spot which exceeds at least 900 μm in a 10-s exposure. A marginal carbonization zone of 30 μm width seems tolerable for microsurgical applications. Coagulation can be further reduced with superficial cooling. In the femtosecond-pulsed laser experiments performed by Armstrong et al.[38] pulses of less than 10 ps generated photoablation without linear absorption by the target tissue, which is largely due to the shorter exposure time and the characteristics of multiphoton absorption. With respect to ablation speed, Armstrong et al. used a comparatively low pulse rate of 10 Hz. If the pulse rate were raised to 1 kHz, an ablation volume per second of 1.6 mm^3/s can be obtained. In our experiment we used a pulse repetition rate of 1 kHz while the beam diameter was 36 μm resulting in an ablation volume of 0.16 mm^3/s. Although the ablated volume was much smaller, the scanner beam course was not adapted to the specific ablation process and must be optimized further. The findings of the femtosecond ablation series in our study suggest that there is a debris zone, which is most likely due to deposition of bony material following photoablation (Table 2). However, the coagulation effects in our nanosecond-pulsed experiments are less than those observed in cw laser systems that emit in the visible light range, i.e., the KTP at 532 nm and the Argon at 488 nm or 514 nm (Refs. 4, 5, 7, 8, and 13–18). Although pressure transients have not been measured as part of this study, the short duration and low energy of pulses could contribute to avoid acoustic trauma to the outer and inner hair cells. Pfander[42] reported that the likelihood of acoustic trauma is not only dependent on the magnitude of mechanical impact as expressed in decibels, but also on its duration. The absolute limit of tolerable sound pressure level, irrespective of its duration, is estimated at 160 dB(A). As Pratisto et al.[19] pointed out, Erbium:YAG lasers create pulses in the 200-μs range, with superposed peaks of 2-μs duration. Although his group as well as Lippert et al.[21] could not demonstrate any detrimental effect on hearing in their experimental and clinical setting, Häusler et al.[20] warned that a temporary hearing threshold shift of 10 and 33 dB on average did occur 2 h postoperatively in patients who had undergone Erbium:YAG laser stapedotomy. Häusler concluded that single pulses of 20 to 40 mJ, corresponding to fluences of 14 to 28 J/cm^2 could lead to a temporary threshold shift (TTS) of hearing level and recommended to keep fluences in the range of 10 to 17 J/cm^2. Later studies performed by Keck et al.,[22,23] which followed these recommendations, did not observe any persistent postoperative sensorineural hearing loss.

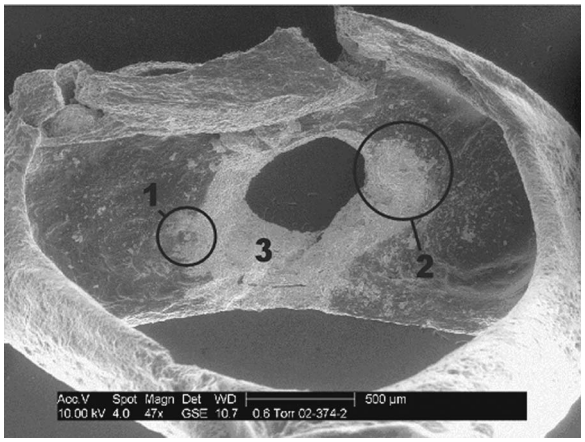

Fig. 8 Comparison of single pulse ablations at 10 mJ (1), 25 mJ (2), and a group of 49 pulses at 15 mJ (3), which created a hole of 400 μm in diameter into a human stapes footplate.

Superficial cooling has been recognized as relevant for the ablation process, especially in exposure times longer than 0.5 s, and if applied, denaturation of adjacent structure is reduced to 30 μm or less. Although fluences in our study were set in the range between 10 and 320 J/cm^2, the laser beam diameter and therefore the exposed areas are very small, thus, decreasing the pressure impact on the inner ear as a whole. In addition, the beam diameter of 10 to 20 μm enhances spatial

Table 2 Comparison of laser parameters and results between Armstrong et al.[38] Schwab et al.[39] our study.

Authors	Year	Laser System	Laser System Parameters	Ablation Characteristics
Armstrong et al.[38]	2002	Ti:sapphire 1053 nm	Pulse energy 2.5 mJ Beam diameter 0.5 mm Fluence 3.2 J/cm^2 (peak) Repetition rate 10 Hz Pulse duration 350 fs	Experimental design Ablation rate (estimate): 1.26 μm per pulse at 1 J/cm^2 (at 1 kHz repetition rate→1 mm/s ablation speed) (Er:YAG 20 to 30 μm/pulse at 10 J/cm^2) (Ho:YAG <0.5to >2.0 μm/pulse) (excimer 2 to 7 μm/pulse)
Schwab et al.[39]	2004	Ti:SAF 780 nm	Pulse energy 1 μJ to 1 mJ Fluence 0.7 J/cm^2 at 130 fs Beam diameter 60 μm Repetition rate 1.04 kHz Pulse duration 130 fs to 1 ps	Ablation rate ~130 nm/pulse at 40-μJ pulse energy and 180 fs pulse duration
Ilgner Wehner et al.	2005	Frequency-tripled Nd:YAG 355 nm	Power 0.16 W Pulse energy 16 nJ Fluence 10.2 J/cm^2	Velocity 200 mm/s Scan time 20 s
Ilgner Wehner et al.	2005	Frequency-tripled Nd:YAG 355 nm	Power 1.5 W Pulse energy 150 nJ Fluence 95.4 J/cm^2	Velocity 500 mm/s Scan time 8 s
Ilgner Wehner et al.	2005	CrLiSAF+Colquerite amplifier 850 nm ±26 nm FWHM	Pulse energy 40 μJ Fluence 3.9 J/cm^2 Beam diameter 36 μm Repetitionrate 1 kHz Pulse duration 100 fs	10 courses at 2 mm/s dz=2 μm/scan Ablation depth 300 μm 1 course at 2 mm/s dz=2 μm/scan ablation depth 40 μm 3 courses at 2 mm/s dz=40 μm/scan Ablation depth 110 μm Duration 40 s/course 10 courses at 2 mm/s dz=40 μm/scan Ablationdepth 300 μm Strong debris

precision, so that the use of a scanning system is favorable, especially in contrast to ablation with commercially available Er:YAG laser systems for ear surgery, which produce a beam diameter that comes close to the required size of the perforation. Scanners for otologic laser procedures are already commercially available, and with greater precision for the drilling procedure, create a better fit of the stapes prosthesis in the stapes footplate and thus reduce the risk of postoperative perilymph leakage from the inner ear. As in our series, scan velocities of 200 to 500 mm/s resulted in superficial to full thickness ablation of the malleus process (about 900 μm) within 20 and 8 s, respectively, the total operation time at the open inner ear is much less than with manual appli-

cation of single pulses in one circle (the so-called "rosette" technique).

Finally, frequency-tripled Nd:YAG lasers are less complex than ultrafast oscillator-amplifier lasers, easier to build, and require less complicated optical devices to shape laser pulses while preserving the pulse duration characteristics. The currently used laboratory models have a power capability of 10 times the required power and the footprint of the laser head is between $4 \times 12 \times 12$ and $4 \times 5 \times 33$ in. When downsizing to the required power level and with further miniaturization, an affordable and rugged operating theater laser unit can be built.

References

1. J. Sataloff, "Experimental use of laser in otosclerotic stapes," *Arch. Otolaryngol.* **85**, 614–616 (1967).
2. T. Palva, "Argon laser in otosclerosis surgery," *Acta Oto-Laryngol.* **104**, 153–157 (1979).
3. R. C. Perkins, "Laser stapedotomy for otosclerosis," *Laryngoscope* **90**, 228–241 (1980).
4. T. M. McGee, "The Argon laser in surgery for chronic ear disease and otosclerosis," *Laryngoscope* **93**, 1177–1182 (1983).
5. J. B. Causse, S. Gherini, and K. J. Horn, "Surgical treatment of stapes fixation by fiberoptic Argon laser stapedotomy with reconstruction of the annular ligament," *Otolaryngol. Clin. North Am.* **26**(3), 395–415 (1993).
6. R. Häusler, A. Messerli, V. Romano, R. Burkhalter, H. P. Weber, and H. J. Altermatt, "Experimental and clinical results of fiberoptic Argon laser stapedotomy," *Eur. Arch. Otorhinolaryngol.* **253**, 193–200 (1996).
7. S. G. Lesinski and A. Palmer, "Lasers for otosclerosis: CO_2 vs. Argon and KTP-532," *Laryngoscope* **99**, 1–8 (1989).
8. S. G. Lesinski and J. A. Stein, "Stapedectomy revision with the CO_2 laser," *Laryngoscope* **99**, 13–19 (1989).
9. S. Jovanovic, D. Anft, U. Schönfeld, A. Berghaus, and H. Scherer, "Animal experimental studies on CO_2 laser stapedotomy," *Laryngol., Rhinol., Otol.* **74**, 26–32 (1995).
10. E. Lescanne, S. Moriniere, C. Gohler, A. Manceau, P. Beutter, and A. Robier, "Retrospective case study of carbon dioxide laser stapedotomy with lens-based and mirror-based micromanipulators," *J. Laryngol. Otol.* **117**, 256–260 (2003).
11. G. Motta and L. Moscillo, "Functional results in stapedotomy with and without CO_2 laser," *ORL* **64**, 307–310 (2002).
12. S. G. Lesinski and R. Newrock, "Carbon dioxide lasers for otosclerosis," *Otolaryngol. Clin. North Am.* **26**(3), 417–441 (1993).
13. H. Silverstein, S. Rosenberg, and R. Jones, "Small fenestra stapedotomies with and without KTP laser: a comparison," *Laryngoscope* **99**, 485–488 (1989).
14. L. J. Bartels, "KTP laser stapedotomy: is it safe?," *Otolaryngol.-Head Neck Surg.* **103**, 685–692 (1990).
15. E. M. Michaelides and J. M. Kartush, "Implications of sound levels generated by otologic devices," *Otolaryngol.-Head Neck Surg.* **125**, 361–363 (2000).
16. R. Mills, M. Szymanski, and E. Abel, "Delayed facial palsy following laser stapedectomy: in vitro study of facial nerve temperature," *Clin. Otolaryngol.* **28**, 211–214 (2003).
17. S. G. Lesinski, "Revision stapedectomy," *Curr. Opin. Otolaryngol. Head Neck Surg.* **11**, 347–354 (2003).
18. M. Szymanski, R. Mills, and E. Abel, "Transmission of heat to the vestibule during revision stapes surgery using a KTP laser: an in vitro study," *J. Laryngol. Otol.* **117**, 349–352 (2003).
19. H. Pratisto, M. Frenz, M. Ith, V. Romano, M. Felix, R. Grossenbacher, H. J. Altermatt, and H. P. Weber, "Temperature and pressure effects during Erbium laser stapedotomy," *Lasers Surg. Med.* **18**, 100–108 (1996).
20. R. Häusler, P. J. Schär, H. Pratisto, H. P. Weber, and M. Frenz, "Advantages and dangers of Erbium:YAG laser application in stapedotomy," *Acta Oto-Laryngol.* **119**, 207–213 (1998).
21. B. M. Lippert, S. Gottschlich, C. Külkens, B. J. Folz, H. Rudert, and J. A. Werner, "Experimental and clinical results of Er:YAG laser stapedotomy," *Lasers Surg. Med.* **28**, 11–17 (2001).
22. T. Keck, M. Wiebe, G. Rettinger, and H. Riechelmann, "Safety of the Erbium:yttrium-aluminium-garnet laser in stapes surgery in otosclerosis," *Otol. Neurotol.* **23**, 21–24 (2002).
23. T. Keck, M. Wiebe, H. Riechelmann, and G. Rettinger, "Results after Erbium:YAG-laser stapedotomy," *Laryngol., Rhinol., Otol.* **82**(3), 157–161 (2003).
24. S. Jovanovic, U. Schönfeld, V. Prapavat, A. Berghaus, R. Fischer, H. Scherer, and G. J. Müller, "Effects of pulsed laser systems on stapes footplate," *Lasers Surg. Med.* **21**, 341–350 (1997).
25. S. Jovanovic, Y. Jamali, D. Anft, U. Schönfeld, H. Scherer, and G. Müller, "Influence of pulsed laser irradiation on the morphology and function of the guinea pig cochlea," *Hear. Res.* **144**, 97–108 (2000).
26. M. Kautzky, A. Trödhan, M. Susani, and P. Schenk, "Infrared laser stapedotomy," *Eur. Arch. Otorhinolaryngol.* **248**, 449–451 (1991).
27. D. S. Poe, "Laser-assisted endoscopic stapedectomy: a prospective study," *Laryngoscope* **110**, 1–37 (2000).
28. B. J. F. Wong, J. Neev, and M. J. C. van Gemert, "Surface temperature distributions in carbon dioxide, Argon, and KTP (Nd:YAG) laser ablated otic capsule and calvarial bone," *Am. J. Otol.* **18**, 766–772 (1997).
29. C. L. Strunk and F. B. Quinn, "Stapedectomy surgery in residency: KTP-532 laser versus Argon laser," *Am. J. Otol.* **14**, 113–117 (1993).
30. S. Jovanovic, D. Anft, U. Schönfeld, A. Berghaus, and H. Scherer, "Influence of CO_2 laser application to the guinea pig cochlea on compound action potentials," *Am. J. Otol.* **20**, 166–173 (1999).
31. E. K. Gardner, J. Dornhoffer, and S. Ferguson, "Photoacoustic effects of carbon dioxide lasers in stapes surgery: quantification in a temporal bone model," *Otol. Neurotol.* **23**, 862–865 (2002).
32. P. Garin, S. van Prooyen-Keyser, and J. Jamart, "Hearing outcome following laser-assisted stapes surgery," *J. Otolaryngol.* **31**, 31–34 (2002).
33. R. J. Wiet, D. C. Kubek, P. Lemberg, and A. T. Byskosh, "A meta-analysis review of revision stapes surgery with Argon laser: effectiveness and safety," *Am. J. Otol.* **18**, 166–171 (1997).
34. C. A. Buchman, M. J. Fucci, J. B. Roberson, and A. De La Cruz, "Comparison of Argon and CO_2 laser stapedotomy in primary otosclerosis surgery," *Am. J. Otol.* **21**(4), 227–230 (2000).
35. S. G. Gherini, K. L. Horn, C. A. Bowman, and G. Griffin, "Small fenestra stapedotomy using a fiberoptic hand-held Argon laser in obliterative otosclerosis," *Laryngoscope* **100**, 1276–1282 (1990).
36. S. G. Gherini, K. L. Horn, J. B. Causse, and G. R. McArthur, "Fiberoptic Argon laser stapedotomy: is it safe?" *Am. J. Otol.* **14**(3), 283–289 (1993).
37. J. Neev, J. S. Nelson, M. Critelli, J. L. McCullough, E. Cheung, W. A. Carrasco, A. M. Rubenchik, L. B. Da Silva, M. D. Perry, and B. C. Stuart, "Ablation of human nail by pulsed lasers," *Lasers Surg. Med.* **21**, 186–192 (1997).
38. W. B. Armstrong, J. A. Neev, L. B. Da Silva, A. M. Rubenchik, and B. C. Stuart, "Ultrashort pulse laser ossicular ablation and stapedotomy in cadaveric bone," *Lasers Surg. Med.* **30**, 216–220 (2002).
39. B. Schwab, D. Hanger, W. Müller, H. Lubatschowski, T. Lenarz, and R. Heermann, "Bone ablation using ultrashort laser pulses. A new technique for middle ear surgery," *Laryngol., Rhinol., Otol.* **83**, 219–225 (2004).
40. M. H. Niemz, "Threshold dependence of laser-induced optical breakdown on pulse duration," *Appl. Phys. Lett.* **66**(10), 1181–1183 (1995).
41. J. Noack, D. X. Hammer, G. D. Noojin, B. A. Rockwell, and A. Vogel, "Influence of pulse duration on mechanical effects after laser-induced breakdown in water," *J. Appl. Phys.* **83**(12), 7488–7495 (1998).
42. S. Pfander, *Das Knalltrauma*, pp. 56–80, Springer, Berlin, Heidelberg, New York (1975) (in German).